Primary Realization of Inductance and Capacitance Scales With a Fully Digital Bridge

Primary Realization of Inductance and Capacitance Scales With a Fully Digital Bridge

Martina Marzano, Vincenzo D'Elia, Massimo Ortolano, and Luca Callegaro

***Abstract*— This article describes an automated electronic fully digital bridge for the comparison of four-terminal-pair (4TP) impedance standards in the audio frequency range. The bridge relative accuracy, which is on the order of 10^{-6}, makes it suitable as a reference bridge for the realization of primary scales of inductance and capacitance in metrology institutes and calibration laboratories. The performances of this bridge were validated by comparing the results of the calibrations of inductance and capacitance standards with those obtained from an existing analog reference system based on the three-voltage method. The article also reports the results of this validation.**

***Index Terms*— Bridge circuits, calibration, impedance measurement, measurement errors, measurement uncertainty.**

I. Introduction

TRACEABLE measurements of electrical impedance require the calibration of the meters employed, which, nowadays, are typically *LCR* electronic impedance bridges. The calibration is performed with artifact standards of ac resistance, inductance, and capacitance, and these require calibrations traceable to realizations of the impedance units ohm (Ω), henry (H) and farad (F) within the International System of Units (SI). These units are linked by the SI unit of time, the second (s), by the relations $1\,\Omega = 1\,\mathrm{H\,s^{-1}} = 1\,\mathrm{F^{-1}\,s}$. In the SI, the ohm can be realized from a quantized Hall resistance standard and, therefore, the capacitance and inductance units can be derived from the ohm and the second.

Traditionally, and as proposed in the SI brochure [1, Appendix 2], the farad is realized from the ohm with a *quadrature bridge* [2] at a suitable capacitance level in the nF range, and then scaled up and down with a transformer ratio bridge [3], [4]. Inductance is then realized from capacitance by either a resonance method [5] (in the mH range, and then scaled with a transformer bridge) or a Maxwell–Wien bridge [6]. These kinds of realizations achieve high accuracies but require complex implementations and considerable efforts from highly skilled operators.

Manuscript received 29 May 2022; revised 14 September 2022; accepted 2 October 2022. Date of publication 13 October 2022; date of current version 31 October 2022. This work was supported in part by the European Metrology Programme for Innovation and Research (EMPIR) Program through the Participating States and in part by the European Union's Horizon 2020 Research and Innovation Program. The Associate Editor coordinating the review process was Yasutaka Amagai. *(Corresponding author: Martina Marzano.)*

Martina Marzano, Vincenzo D'Elia, and Luca Callegaro are with the Istituto Nazionale di Ricerca Metrologica (INRIM), 10135 Turin, Italy (e-mail: m.marzano@inrim.it).

Massimo Ortolano is with the Politecnico di Torino, 10129 Turin, Italy, and also with the Istituto Nazionale di Ricerca Metrologica (INRIM), 10135 Turin, Italy.

Digital Object Identifier 10.1109/TIM.2022.3214498

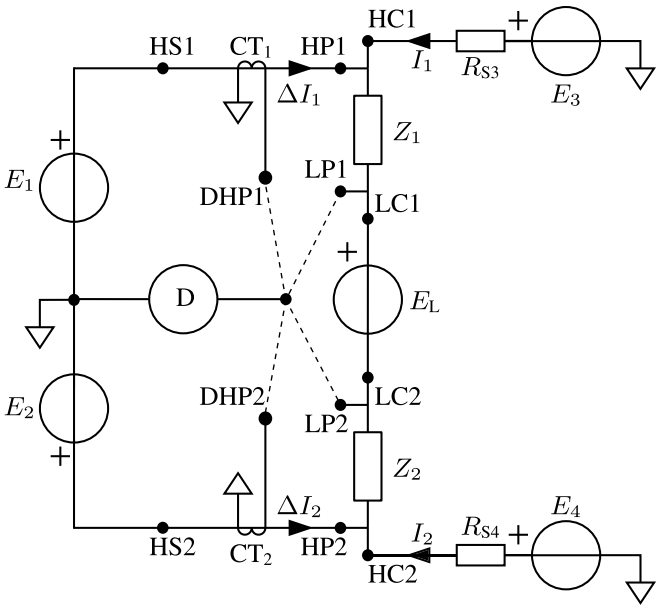

Fig. 1. Basic schematic of the fully digital bridge: Z_1 and Z_2 are the reference standards under comparison, defined as 4TP impedances at the ports HP1, HC1, LP1, and LC1, and HP2, HC2, LP2, and LC2, respectively; the voltage sources E_1, E_2, E_3, E_4, and E_L represent the outputs of a polyphase digital sinewave synthesizer operating at frequency f; R_{S3} and R_{S4} are series resistances injecting current into the high-current ports HC1 and HC2; CT_1 and CT_2 are current transformers measuring the currents ΔI_1 and ΔI_2; the detector D is a lock-in amplifier referenced at f; and LP1, LP2, DHP1, and DHP2 are the detection ports.

Digital impedance bridges, which are based on mixed-signal electronics, have evolved from their original concept [7], [8], [9], [10], [11] to recent implementations [12], [13], [14], [15], [16], [17], [18], [19], [20], [21], [22], [23], [24], [25], [26] providing accuracy and flexibility suitable for the direct realization of inductance and capacitance scales. In particular, electronic *fully digital* impedance bridges [15], [16], [17], [21], [22], [23], [25], [26] do not include calibrated ratio transformers in their implementation but rely on the accuracy of the electronic waveform synthesizers employed. These can be more easily manufactured and operated, thus allowing the developing metrology institutes and calibration centers to realize impedance scales. At the Istituto Nazionale di Ricerca Metrologica (INRIM), the first step toward the use of electronic bridges in the realization of impedance scales was achieved in the 1980s [27], and a second one was achieved about 20 years ago, with an implementation of the *three-voltage method*, [28], [29], [30] and Section III. This method relies on a high-accuracy ac voltmeter and it is assisted by digital electronics, and allowed to achieve an uncertainty of parts in 10^5 or less. However, the operating ranges for fre-

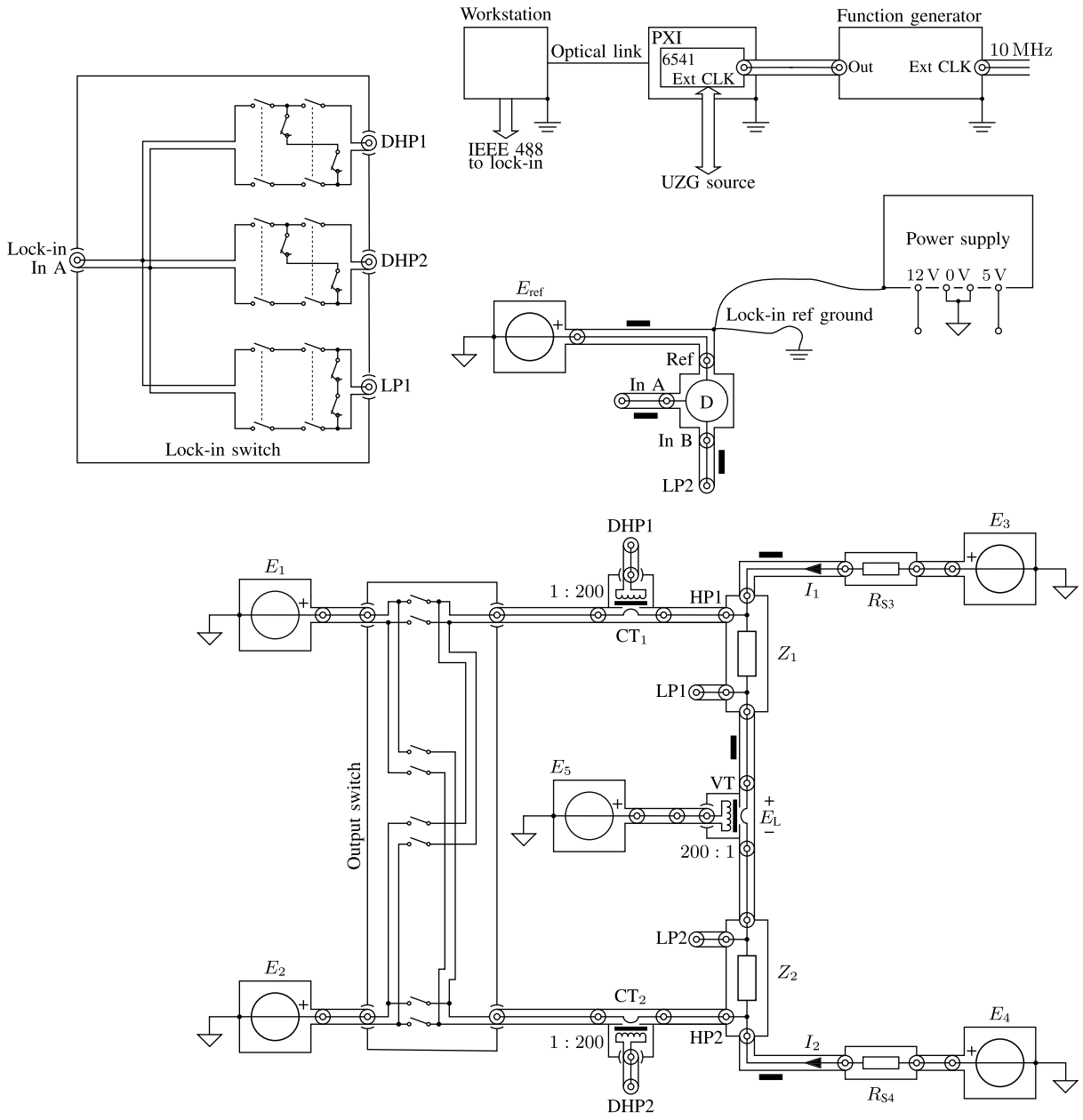

Fig. 2. Coaxial schematic of the fully digital bridge. The solid black marks represent the coaxial equalizers.

quency and impedance magnitude of the three-voltage method are limited. Moreover, the implementation is expensive with a suboptimal level of automation. More recently, INRIM was involved in the development of fully digital bridges [16], [23], [25], [26] in the framework of a number of European joint research projects [31], [32], [33], [34], [35], [36]. In particular, the project VersICaL[1] had the specific objective of developing a new fully digital bridge to be used as a primary reference bridge for the realization of impedance units and scales in national metrology institutes and calibration centers, and for the training of electrical metrologists [37].

This article discusses this new fully digital bridge and its application to the realization of inductance and capacitance scales from the ac resistance scale in a metrology laboratory. This bridge allows the comparison of four-terminal-pair (4TP) impedances in extended magnitude and frequency ranges, with a high level of automation and usability, and is suitable for an industrial uptake toward adoption in calibration centers.

This article reports a comparison between the calibrations performed with the digital bridge and the three-voltage method. This comparison constitutes a validation of the digital bridge and the basis of a future overhaul and extension of the Italian national scales of inductance and capacitance.

II. Fully Digital Bridge

A. Working Principle

A simplified, noncoaxial schematic of the fully digital bridge is shown in Fig. 1. The 4TP [38] impedance standards being compared are Z_1, which we assume to be the reference standard, connected to the bridge ports LC1, LP1, HC1 and HP1, and Z_2, which we assume to be the standard under calibration, connected to the bridge ports LC2, LP2, HC2 and

[1]EMPIR project 17RPT04 VersICal, *A versatile electrical impedance calibration laboratory based on digital impedance bridges*.

HP2. The voltage sources E_1, E_2, E_3, E_4, and E_L correspond to the outputs of a polyphase digital sinewave synthesizer operating at frequency f. The bridge operation is based on the comparison of the impedance ratio Z_1/Z_2 to the main voltage ratio E_1/E_2. The auxiliary voltage sources E_3, E_4, and E_L realize the 4TP impedance definition: E_3 and E_4 generate, through the resistances R_{S3} and R_{S4}, the currents I_1 and I_2 driving Z_1 and Z_2; E_L compensates the voltage across the series impedance between the low potential ports LP1 and LP2 of Z_1 and Z_2, respectively.

The bridge is balanced, and the 4TP definition of the impedances fulfilled, when $V_{LP1} = 0$, $V_{LP1} - V_{LP2} = 0$ and $\Delta I_1 = \Delta I_2 = 0$. The balance is achieved by adjusting the voltages E_2, E_3, E_4, and E_L in magnitude and phase. The voltage E_1 is kept constant to fix the measurement current through the reference standard Z_1.

The balance conditions are checked by detector D, a lock-in amplifier with two inputs A and B, referenced at f. Input A can be connected in turn to the detection ports LP1, DHP1 and DHP2. The ports DHP1 and DHP2 are connected to the transformers CT_1 and CT_2, which detect the residual currents ΔI_1 and ΔI_2. The input B is permanently connected to LP2, and it is used to check the condition $V_{LP1} - V_{LP2} = 0$ by operating D in differential mode with input A connected to LP1.

When the bridge is balanced the impedance ratio is given by

$$W = \frac{Z_1}{Z_2} = -\frac{E_1}{E_2}. \tag{1}$$

The bridge reading is given by the settings E_1^{read} and E_2^{read} of the voltage phasors E_1 and E_2, computed from the samples that synthesize the two sinusoidal waveforms. To cancel the effect of the synthesizer's gain error, the reading is obtained from two successive balances: in the *forward* configuration, the bridge is balanced as in Fig. 1; in the *reverse* configuration, the bridge is balanced with the channels E_1 and E_2 exchanged at the ports HS1 and HS2. The bridge reading is then computed as [16], [24], [26]

$$W^{\text{read}} = W_F^{\text{read}} \sqrt{\frac{W_R^{\text{read}}}{W_F^{\text{read}}}} \tag{2}$$

with

$$W_F^{\text{read}} = -\frac{E_{1F}^{\text{read}}}{E_{2F}^{\text{read}}} \quad \text{and} \quad W_R^{\text{read}} = -\frac{E_{2R}^{\text{read}}}{E_{1R}^{\text{read}}} \tag{3}$$

where E_{1F}^{read}, E_{2F}^{read}, E_{1R}^{read}, and E_{2R}^{read} are the synthesizer's settings in the forward (F subscript) and reverse (R subscript) configurations. The complex square root in (2) should be determined with a positive real part.

B. Implementation

A coaxial schematic of the fully digital bridge is shown in Fig. 2, and a picture in Fig. 3.

1) Synthesizer: The voltage sources from E_1 to E_5 and E_{ref} represent the output channels of a 7-channel polyphase sinewave synthesizer (DSS2A-INRIM) designed and manufactured by the University of Zielona Góra (UZG) [37], [39]. The synthesizer is composed of a digital waveform instrument (National Instruments PXI-6541), and a digital-to-analog converter (DAC) and analog output unit. Each analog channel includes two 18-bit DACs, for the waveform synthesis and the amplitude scaling, low-pass filters and buffers. The output frequency range of the synthesizer is 20 Hz to 20 kHz. At present, the operating frequency range of the fully digital bridge is narrower to some extent, depending on the target uncertainty. At low frequency, the actual limit is around a few tens of hertz, determined by the reduced efficacy of the current equalizers in ensuring the coaxiality of the bridge network; at high frequency, the limit is determined by the reduced balancing resolution (at 20 kHz, the synthesized waves are composed of just 25 samples).

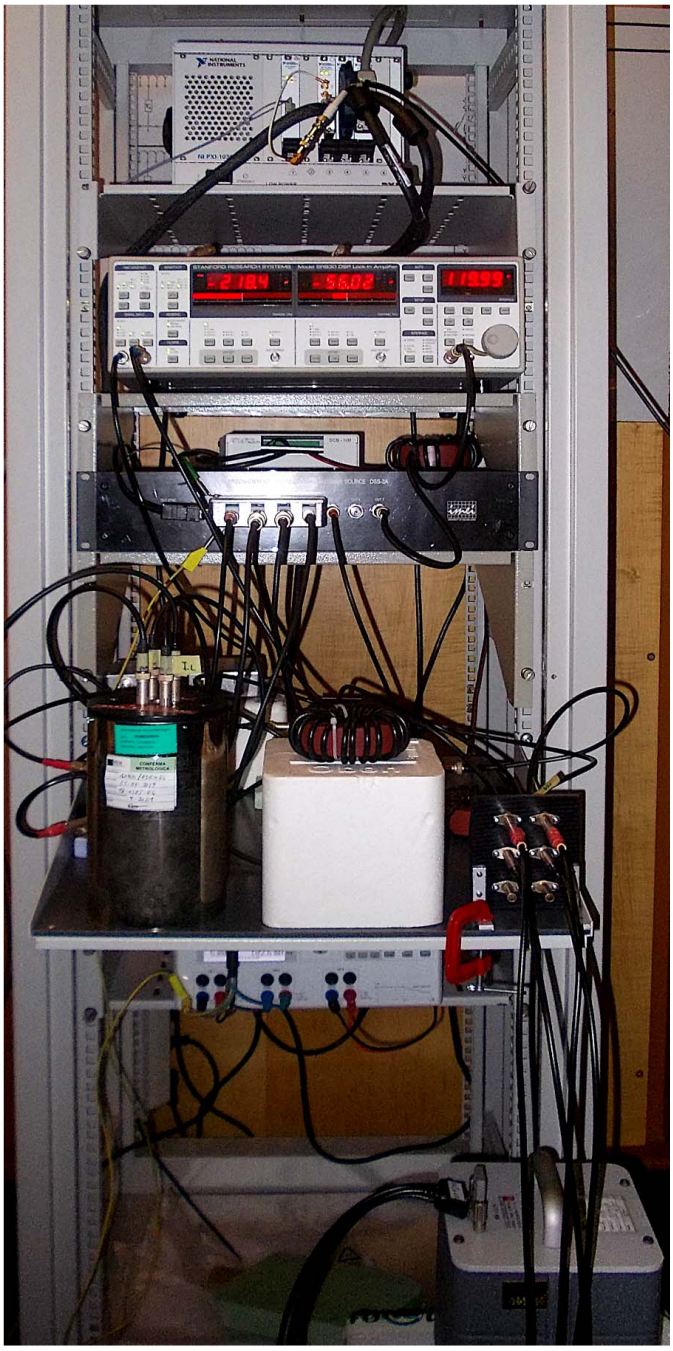

Fig. 3. Photograph of the fully digital bridge (from [26]).

There are four available voltage ranges, 1, 2.5, and 5 V, with a maximum rms output current of 100 mA.

The voltage E_L is obtained from E_5 with an injection transformer VT.

The resistors R_{S3} and R_{S4} are of either 10 Ω or 100 Ω, depending on the magnitudes of Z_1 and Z_2 and the operating current.[2]

2) Detector: The detector is a Stanford Research SR 830 lock-in amplifier, switched between the single-ended and the differential modes of operation. The reference channel is driven at frequency f by the channel E_{ref} of the synthesizer.

3) Switches: There are two coaxial switches. The *output switch* is connected to E_1 and E_2 to implement the forward and reverse configurations. The *lock-in switch* connects the input A of the lock-in amplifier to the various detection ports, according to the balance procedure. Both switches are composed of mechanical relays (Panasonic DS2E-S-5 V) which connect and disconnect both the inner and the outer conductors of each coaxial line. Each channel of the lock-in switch has additional relay contacts to reduce the current leakage through the stray capacitances of the open contacts. The relays are operated by a digital I/O board (National Instruments PXI 6509).

4) Transformers: VT, CT_1, and CT_2 are injection and detection transformers [2] with a 200:1 turns ratio.

5) Current Equalizers: The coaxiality of the bridge network is ensured by six coaxial current equalizers [2], represented by solid black marks in Fig. 2.

6) Software: The bridge control software, described in detail in [37], is based on a client-server architecture. The source code of the client application (BClient) is available online [41]. The server controls the instrumentation (synthesizer, detector, and switches), and the client provides the user interface and implements the balancing algorithm [42]. Both applications are developed with the programming environment National Instruments LabWindows/CVI. The client and the server communicate via a network variable server, supervised by the NI Distributed System Manager, allowing the remote control of the bridge over the Internet.

Associated with the BClient application there is a MATLAB/Octave script (BClientUncertaintyTool) that determines the unknown impedance and the associated uncertainty from the raw data recorded by the BClient application and the reference standard data. This uncertainty tool is also available online [41].

7) Balancing and Measurement Procedure: Starting from the forward configuration shown in Fig. 2, the balancing procedure, which is fully automated by the BClient application, is as follows.

P1. Set E_5 to 0V, and E_1 to the operating value of interest.
P2. Adjust E_3 to null the detector connected to V_{DHP1}.
P3. Adjust E_2 to null the detector connected to V_{LP1}.
P4. Adjust E_4 to null the detector connected to V_{DHP2}.
P5. Adjust E_5 to null the detector reading of the differential voltage $V_{LP1}-V_{LP2}$.
P6. Repeat steps P2 through P5 until the detector is nulled simultaneously within the chosen thresholds for all detection ports.
P7. Record the voltage readings E_{1F}^{read} and E_{2F}^{read}.
P8. Change the setup to the reverse configuration.
P9. Repeat step P2.
P10. Adjust E_1 to null the detector connected to V_{LP1}.
P11. Repeat steps P4 and P5.
P12. Repeat steps P9 through P11 until the detector is nulled simultaneously within the chosen thresholds for all detection ports.
P13. Record the voltage readings E_{1R}^{read} and E_{2R}^{read}.

The ratio W can then be computed from (2) and (3), and the unknown capacitance C_2^{FD} or the unknown inductance L_2^{FD} (Section V) can be determined from W and the reference impedance Z_1.

C. Uncertainty

A detailed analysis of the bridge error sources is presented in [26]. These are as follows.

1) Synthesizer nonlinearity.
2) Synthesizer crosstalk.
3) Loading.
4) Imperfect low balance.
5) Imperfect high balance.

Each of these contributions is dependent on the impedance values, the operating current, the operating frequency, the chosen ranges for the synthesizer's channels, and the balance thresholds. Giving an expression of the uncertainty for the full operating range is impractical because it requires extensive and time-consuming characterization of the synthesizer over several different parameters, and it depends also on the balancing parameters chosen by the operator and their optimization. Partial characterization of the synthesizer for magnitude ratios and frequencies different from those used in this work is reported in [26]. Qualitatively speaking, the main uncertainty component, which is the synthesizer nonlinearity, increases significantly for impedance magnitude ratios greater than about 3:1 or less than 1:3, but is not significantly affected by the operating current because the voltage channels work unloaded. In the comparison of impedances having equal nominal values, the fully digital bridge achieves a relative accuracy of 10^{-6} or less.

Indeed, in addition to the above listed bridge-specific uncertainty sources, the uncertainty of the reference standard Z_1 should also be considered.

Since all quantities involved in the measurement model described in [26] are complex, the uncertainty evaluation should be performed according to [43]. The MATLAB/Octave uncertainty tool [41] provides the uncertainty evaluation for the bridge by propagating the distributions of the complex quantities by means of a Monte Carlo method [43], [44].

Table I reports an example uncertainty budget for the measurement of a 10 mH inductance standard against a 100 Ω resistance standard taken as reference. The Monte Carlo evaluation was performed with a sample size of 10^6.

[2]During the measurement, large capacitive loads that can possibly induce self-oscillations [40] can be isolated with resistors in series with E_1 and E_2. With the standards measured here, this was not necessary.

TABLE I

UNCERTAINTY BUDGET FOR THE FULLY DIGITAL BRIDGE FOR THE COMPARISON OF AN INDUCTANCE STANDARD $L_2 = 10$ mH AGAINST A RESISTANCE STANDARD $R_1 = 100\ \Omega$. RSS IS THE ROOT SUM OF SQUARES OF THE UNCERTAINTY COMPONENTS

Quantity	x_i	$u(x_i)$	Type	Distr.	$u_i(L_2^{\mathrm{FD}})$/nH	Remarks
R_1^{dc}	99.998 72 Ω	0.000 13 Ω	B	Rect.		DC calibration
a_1	1.9×10^{-6}	4.1×10^{-6}	B	Rect.		AC-DC coefficient from AC calibration
τ_1	20 ns	2 ns	B	Rect.		Time constant from AC calibration
Z_1					46	Combined contribution of R_1, a_1 and τ_1
W^{read}	−1.563 877 9	2×10^{-7}	A	Norm.	2	Evaluated with 6 repeated measurements
ΔW_{nl}	0	1.7×10^{-6}	B	Rect.	11	Synthesizer nonlinearity from calibration with IVD
ΔW_{ld}	0	7.0×10^{-7}	B	Rect.	4	Loading error
ΔW_{ct}	0	1.7×10^{-7}	B	Rect.	1	Channel-to-channel crosstalk
L_2^{FD}	9.995 387 mH				48	RSS

TABLE II

COMPARISON OF THE FULLY DIGITAL BRIDGE AND THE THREE-VOLTAGE METHOD IN THE MEASUREMENT OF INDUCTANCE STANDARDS. THE SUBSCRIPT R IS USED TO DENOTE RELATIVE UNCERTAINTIES

L_2	R_1	f	I	$u_{\mathrm{R}}(L_2^{\mathrm{FD}})$ / μH H^{-1}	$u_{\mathrm{R}}(L_2^{3\mathrm{V}})$ / μH H^{-1}	δ / μH H^{-1}	$U_{\mathrm{R}}(\delta)$ / μH H^{-1}
1 mH	10 Ω	1 kHz	50 mA	11.0	15.0	3.8	33.6
10 mH	100 Ω	1 kHz	10 mA	4.8	9.0	1.9	16.2
100 mH	1 kΩ	1 kHz	2 mA	3.8	8.0	-1.6	13.2
1 H	10 kΩ	1 kHz	200 μA	6.5	8.0	0.8	11.1
10 H	10 kΩ	120 Hz	200 μA	6.8	9.0	-14.0	25.0

The main sources of uncertainty are the reference standard, and the synthesizer nonlinearity. The synthesizer nonlinearity was estimated by generating reference voltage ratios with an inductive voltage divider. The type A uncertainty was evaluated with six repeated measurements (other longer measurements yielded similar results) and it includes the effect of imperfect low and high balances.

The combined relative uncertainty of the measured inductance L_2^{FD} is $u_{\mathrm{R}}(L_2^{\mathrm{FD}}) = u(L_2^{\mathrm{FD}})/L_2^{\mathrm{FD}} \approx 4.8$ μH/H.

III. THREE-VOLTAGE METHOD

The three-voltage method was originally developed for measuring electrical power and energy [45], [46], and applied to primary impedance metrology by Cabiati [47], [48], [49].

The principle of the method is described in [28]. As in the fully digital bridge, the impedance standards Z_1 and Z_2 being compared are in series and driven by the same current I. The voltages across Z_1 and Z_2 are $V_1 = Z_1 I$ and $V_2 = -Z_2 I$, respectively. The average voltage $V_{\mathrm{M}} = (V_1 + V_2)/2$ of the phasors V_1 and V_2 is generated with a precision inductive voltage divider set at a fixed ratio of 0.5. The voltage magnitudes $|V_1|$, $|V_2|$ and $|V_{\mathrm{M}}|$ are measured with a precision rms voltmeter. The relevant phasors form closed triangles whose angles can be computed by trigonometry from their sides, that is, from the phasor magnitudes [2]. The resulting measurement model is nonlinear and the uncertainty expression involved [49].

The INRIM implementation is described in [28], [29], and [30]. The impedances Z_1 and Z_2 are driven by digital waveform generators, and custom electronics including both slave digital generators [50] and analog synchronous filters [51] define the standards as 4TP impedances. A single high-accuracy thermal voltmeter (Fluke 5790A) is switched between the three measurand voltages, such that only its linearity enters in the uncertainty budget [52].

The accuracy of the system was validated by international intercomparisons [29], [30].

A drawback of the three-voltage method is a degradation of its performances in doing measurements at the low voltages needed to measure low impedances. One issue is the voltage noise. In fact, the rms voltmeter is wideband and hence prone to interferences, in particular those at the power line frequency and its harmonics. The performances reported in Section V are achieved in a shielded room. Another issue is the poor linearity of the rms voltmeter in the low voltage ranges. The analog electronics employed for the impedance definition have a limited frequency bandwidth (120 Hz to a few kHz) and manual gain ranges. The implementation relies on expensive commercial instruments (mainly the top-class voltmeter and the inductive voltage divider).

IV. REALIZATION OF INDUCTANCE AND CAPACITANCE SCALES

INRIM is a participant of the International Committee for Weights and Measures (CIPM) mutual recognition arrangement [53] and maintains declarations on calibration and measurement capabilities (CMCs), registered in the key comparison database (KCDB) [54]. The CMCs of interest for this article belong to services 4.3 *Inductance: self inductance* and 4.2 *Capacitance: dielectric capacitors*.

The inductance and capacitance scales corresponding to these services are realized with traceability to ac resistance.

The specific artifact standards considered in this work are involved in these scales and are described below. The two-terminal (2T), three-terminal (3T) and two-terminal-pair (2TP) standards are either re-encased as 4TP standards or a 3T-to-4TP adapter is used during the measurements.

A. AC Resistance

The ac resistance scale considered in this work is maintained by Wilkins resistors [55], in particular Tinsley 5685 4T resistance standards with nominal values 10 Ω, 100 Ω, 1 kΩ, and 10 kΩ, encased in shielding boxes provided with

TABLE III
COMPARISON OF THE FULLY DIGITAL BRIDGE AND THE THREE-VOLTAGE METHOD IN THE MEASUREMENT OF CAPACITANCE STANDARDS

C_2	R_1	f	I	$u_R(C_2^{FD})$ / μF F^{-1}	$u_R(C_2^{3V})$ / μF F^{-1}	δ / μF F^{-1}	$U_R(\delta)$ / μF F^{-1}
10 nF	10 kΩ	1 kHz	130 μA	8.8	8.0	6.9	17.3
100 nF	1 kΩ	1 kHz	630 μA	7.4	7.0	3.7	17.1
1 μF	100 Ω	1 kHz	3.175 mA	7.9	8.5	12.0	17.1
10 μF	10 Ω	1 kHz	32.5 mA	7.1	17.0	-15.0	22.2
100 μF	10 Ω	120 Hz	40 mA	7.2	18.0	0.5	25.3

internal adapters from the original four-terminal connections to 4TP British Post Office Multiple Unit Steerable Array (BPO-MUSA) connectors. The dc resistance is periodically calibrated by 1:1 comparisons against the national dc resistance standard [56]. The ac–dc coefficient and the time constant were evaluated during an international intercomparison [57].

B. Inductance

The inductance scale considered in this work is maintained with commercial air-core toroidal self-inductors, with nominal values 1 mH, 10 mH, 100 mH, 1 H, and 10 H, defined as 2T or 3T standards. All standards belong to the General Radio/IET Labs 1482 series. To perform the measurements with the fully digital bridge or the three-voltage setup, the original 2T or 3T definition is converted to the 4TP definition with a special adapter having minimal stray parameters, and which was proven to introduce negligible effect in the course of an international intercomparison [58].

C. Capacitance

The capacitance scale from 10 nF to 100 μF is maintained with a set of solid-dielectric capacitors (ceramic C0G Novacap NOV01 2T 10 nF; mica H. W. Sullivan 2TP 100 nF and 1 μF; polypropylene SCR PA 1000 and 10 000, respectively, 2T 10 and 100 μF capacitance standards). All the standards are re-encased as 4TP and the 10 nF thermostated capacitor was described in [59].

D. Environment

The fully digital bridge, the three-voltage setup and the standards are operated and maintained in a shielded room, thermostated at (23.0 ± 5) °C.

V. COMPARISON

Validation of the fully digital bridge was performed by taking the three-voltage setup as a reference. Both systems were employed to perform calibrations of an inductance or a capacitance standard Z_2 against a resistance standard R_1 taken as reference.

The list of comparisons is shown in Table II for the inductance standards and in Table III for the capacitance standards. The nominal values and frequencies of the comparisons are limited to the nominal values and frequencies covered by the three-voltage method and for which CMCs have been declared in the KCDB.

The first sections of Tables II and III (columns 1–4) report the measurand nominal value (L_2 or C_2, respectively), the reference impedance R_1, the measurement frequency f and the rms current I. The resistor nominal value R_1 is chosen, from the available decadal values, to have an impedance magnitude ratio $|Z_2/Z_1|$ as close as possible to 1. For each pair of standards, the measurement with the fully digital bridge (L_2^{FD} or C_2^{FD}) and the one with the three-voltage method (L_2^{3V} or C_2^{3V}, taken as reference) are performed in close time succession, to minimize the effect of possible thermal or time drifts.[3]

The second sections of the tables (columns 5 and 6) report the 1-σ relative uncertainties of the two measurements, denoted by the subscript R. For the fully digital bridge, $u_R(L_2^{FD})$ and $u_R(C_2^{FD})$ are evaluated as in Section II-C. For the three-voltage method, $u_R(L_2^{FD})$ and $u_R(C_2^{FD})$ are evaluated as in [28] and published in the KCDB [54]. These uncertainties include the contribution of the reference impedance Z_1 and thus give the performances of the two systems when employed in regular calibrations.

The third section of the table (columns 6 and 7) reports the result of the comparison δ, that is, the relative difference between the values of L_2 or C_2 measured by the two instruments, and its 2-σ expanded relative uncertainty $U_R(\delta)$. This uncertainty is evaluated by considering the values of the reference impedance Z_1 as totally correlated between the two measurements. Hence, the corresponding uncertainty $u(Z_1)$ is not included in this calculation.

As Tables II and III show the values obtained with the two systems are compatible within the expanded relative uncertainty. The measured series resistances of the inductance standards are also compatible with most measurements but not reported in Table II for brevity. The measured dissipation factors of the capacitance standards were not compared because highly unstable.

VI. CONCLUSION

The results given in Tables II and III mutually validate the performances of the two instruments in their common working magnitude and frequency range, which is limited by the three-voltage method. The fully digital bridge achieves lower uncertainty in most measurements and overcomes the performance limitations of the three-voltage method (Section III).

Further characterizations of the fully digital bridge are ongoing to determine its performances in the magnitude and frequency ranges not covered by the three-voltage method.

[3] All measurements were performed in a shielded and thermostated room at (23.0 ± 5) °C. Since air-core inductors have a significant inductance temperature coefficient (30×10^{-6}/K), the 1 mH and 10 mH standards were further placed in a thermostated chamber with temperature stability of 4 mK. The 100 mH standard has an independent thermostat [60]. Even though small corrections can be performed to the readings on the basis of the equivalent series resistance, as suggested by the manufacturer [61], none were deemed necessary.

The new fully digital bridge is fully automated, can be operated remotely, and was the basis of a training program of European metrologists [37]. A bridge based on this design has been implemented at the National Standards Authority of Ireland (NSAI), the Irish metrology institute. The commercial instruments employed for the bridge implementation (Section II-C) can be replaced with purposely designed electronics on the road toward an industrial product and to extend its use in calibration laboratories. The validation of the bridge reported in this article is the main step toward its formal adoption in the Italian national standard and scales of inductance and capacitance, and the improvement of the Italian calibration and measurement capabilities.

The accuracy of the inductance and capacitance scales realized with the new fully digital bridge is now limited by the accuracy of the available ac resistance scale which is limited by the knowledge of the frequency and phase angle dependence of the artifact resistance standards employed. A set of Gibbings [62] calculable resistors, having values of 100 Ω, 1 kΩ, 10 kΩ, and 12 906.4 Ω is already available. Their frequency dependence can be calculated with uncertainty in the 10^{-8} range for the ac–dc deviation and of about 1 ns for the time constant at 1 kHz. They will be characterized and put into service to partially replace the existing resistor set, thus improving the uncertainty of all the three impedance scales of ac resistance, inductance, and capacitance.

ACKNOWLEDGMENT

The authors are indebted to Danilo Serazio, INRIM, who constructed several electromagnetic devices employed in the experiment, and Dario Pilori, together with the INRIM IT help desk, for the contribution to the networking of the fully digital bridge. The work has been realized within the Joint Research Project 17RPT04 VersICaL: *A versatile impedance calibration laboratory based on digital impedance bridges*.

REFERENCES

[1] *The International System of Units*, Bureau International des Poids et Mesures, Sèvres, France, 9th ed. 2019. [Online]. Available: https://www.bipm.org

[2] L. Callegaro, *Electrical Impedance: Principles, Measurement, and Applications* (Series in Sensors). Boca Raton, FL, USA: CRC Press, 2013.

[3] B. P. Kibble and G. H. Rayner, *Coaxial AC bridges*. Bristol, U.K.: Adam Hilger, 1984.

[4] S. Awan, B. Kibble, and J. Schurr, *Coaxial Electrical Circuits for Interference-Free Measurements* (Electrical Measurement Series). London, U.K.: The Institution of Engineering and Technology, 2011.

[5] G. H. Rayner, B. P. Kibble, and M. J. Swan, "On obtaining the Henry from the Farad," NPL Report, Teddington, U.K., Tech. Rep. DES 63, Mar. 1980.

[6] B. Hague, *Alternating Current Bridge Methods*, 6th ed. London, U.K.: Pitman Publishing, 1971.

[7] G. Trenkler, "Digitalmeßbrücke zum vergleich von wirk-und blindwiderständen," *Technisches Messen*, vols. 503–513, no. 1, pp. 313–314, May 1978, doi: 10.1524/teme.1978.503513.jg.313.

[8] H. Bachmair and R. Vollmert, "Comparison of admittances by means of a digital double-sinewave generator," *IEEE Trans. Instrum. Meas.*, vol. IM-29, no. 4, pp. 370–372, Dec. 1980.

[9] W. Helbach, P. Marczinowski, and G. Trenkler, "High-precision automatic digital Ac bridge," *IEEE Trans. Instrum. Meas.*, vol. IM-32, no. 1, pp. 159–162, Mar. 1983.

[10] H. Schollmeyer, "A digital AC bridge as an impedance to frequency converter," *IEEE Trans. Instrum. Meas.*, vol. IM-34, no. 3, pp. 389–392, Sep. 1985.

[11] W. Helbach and H. Schollmeyer, "Impedance measuring methods based on multiple digital generators," *IEEE Trans. Instrum. Meas.*, vol. IM-36, no. 2, pp. 400–405, Jun. 1987.

[12] B. Trinchera, L. Callegaro, and V. D'Elia, "Quadrature bridge for *R-C* comparisons based on polyphase digital synthesis," *IEEE Trans. Instrum. Meas.*, vol. 58, no. 1, pp. 202–206, Aug. 2009. [Online]. Available: http://ieeexplore.ieee.org/document/4601488/

[13] L. Callegaro, V. D'Elia, and B. Trinchera, "Realization of the Farad from the DC quantum Hall effect with digitally assisted impedance bridges," *Metrologia*, vol. 47, no. 4, pp. 464–472, 2010.

[14] F. Overney and B. Jeanneret, "Realization of an inductance scale traceable to the quantum Hall effect using an automated synchronous sampling system," *Metrologia*, vol. 47, no. 6, pp. 690–698, Dec. 2010.

[15] F. Overney and B. Jeanneret, "*RLC* bridge based on an automated synchronous sampling system," *IEEE Trans. Instrum. Meas.*, vol. 60, no. 7, pp. 2393–2398, Jul. 2011.

[16] L. Callegaro, V. D'Elia, M. Kampik, D. B. Kim, and M. Ortolano, "Experiences with a two-terminal-pair digital impedance bridge," *IEEE Trans. Instrum. Meas.*, vol. 64, no. 6, pp. 1460–1465, Jun. 2015.

[17] W. G. K. Ihlenfeld and R. T. B. Vasconcellos, "A digital four terminal-pair impedance bridge," in *Proc. Conf. Precis. Electromagn. Meas. (CPEM)*, Ottawa, ON, Canada, Jul. 2016, pp. 1–2.

[18] F. Overney et al., "Josephson-based full digital bridge for high-accuracy impedance comparisons," *Metrologia*, vol. 53, no. 4, pp. 1045–1053, 2016.

[19] S. Bauer et al., "A novel two-terminal-pair pulse-driven Josephson impedance bridge linking a 10 nF capacitance standard to the quantized Hall resistance," *Metrologia*, vol. 54, no. 2, pp. 152–160, 2017.

[20] T. Hagen, L. Palafox, and R. Behr, "A Josephson impedance bridge based on programmable Josephson voltage standards," *IEEE Trans. Instrum. Meas.*, vol. 66, no. 6, pp. 1539–1545, Jun. 2017.

[21] J. Kucera and J. Kováč, "A reconfigurable four terminal-pair digitally assisted and fully digital impedance ratio bridge," *IEEE Trans. Instrum. Meas.*, vol. 67, no. 5, pp. 1199–1206, May 2018.

[22] F. Overney and B. Jeanneret, "Impedance bridges: From wheatstone to Josephson," *Metrologia*, vol. 55, no. 5, pp. S119–S134, Oct. 2018.

[23] M. Ortolano et al., "An international comparison of phase angle standards between the novel impedance bridges of CMI, INRIM and METAS," *Metrologia*, vol. 55, no. 4, pp. 499–512, 2018.

[24] F. Overney et al., "Dual Josephson impedance bridge: Towards a universal bridge for impedance metrology," *Metrologia*, vol. 57, no. 6, pp. 1–18, 2020.

[25] M. Marzano, M. Ortolano, V. D'Elia, A. Müller, and L. Callegaro, "A fully digital bridge towards the realization of the Farad from the quantum Hall effect," *Metrologia*, vol. 58, no. 1, Dec. 2020, Art. no. 015002.

[26] M. Ortolano et al., "A comprehensive analysis of error sources in electronic fully digital impedance bridges," *IEEE Trans. Instrum. Meas.*, vol. 70, pp. 1–14, 2021.

[27] F. Cabiati and G. C. Bosco, "LC comparison system based on a two-phase generator," *IEEE Trans. Instrum. Meas.*, vols. IM-34, no. 2, pp. 344–349, Jun. 1985.

[28] L. Callegaro and V. D'Elia, "Automated system for inductance realization traceable to AC resistance with a three-voltmeter method," *IEEE Trans. Instrum. Meas.*, vol. 50, no. 6, pp. 1630–1633, Dec. 2001.

[29] L. Callegaro, "EUROMET.EM-S20: Intercomparison of a 100 mH inductance standard (Euromet project 607)," *Metrologia*, vol. 44, no. 1A, 2007, Art. no. 01002.

[30] L. Callegaro, V. D'Elia, and J. Bohacek, "Four-terminal-pair inductance comparison between INRIM and CTU," *IEEE Trans. Instrum. Meas.*, vol. 58, no. 1, pp. 87–93, Jan. 2009.

[31] (2015). *EMPIR Joint Research Project 17RPT04 VersICaL, A Versatile Electrical Impedance Calibration Laboratory Based on Digital Impedance Bridges*. [Online]. Available: https://sites.google.com/inrim.it/versical.nrim.it/versical

[32] L. Palafox et al., "AIM QuTE: Automated impedance metrology extending the quantum toolbox for electricity," in *Proc. 16th Int. Congr. Metrol.*, 2013, p. 11001.

[33] (2018). *EMRP Joint Research Project SIB53 AIM QuTE, Automated Impedance Metrology Extending the Quantum Toolbox for Electricity*. [Online]. Available: https://sites.google.com/inrim.it/versical

[34] O. Power et al., "Practical precision electrical impedance measurement for the 21st century—EMPIR project 17RPT04 VersICal," in *Proc. 19th Int. Congr. Metrol. (CIM)*, 2019, Art. no. 02001, doi: 10.1051/metrology/201902001.

[35] *EMPIR Joint Research Project 18SIB07 GIQS, Graphene Impedance Quantum Standard*, [Online]. Available: https://www.ptb.de/empir2019/giqs

[36] L. Callegaro et al., "The EMPIR project GIQS: Graphene impedance quantum standard," in *Proc. Conf. Precis. Electromagn. Meas. (CPEM)*, 2020, pp. 1–2.
[37] "A versatile electrical impedance calibration laboratory based on digital impedance bridges (VersICaL)," Final Publishable Report, EMPIR Project 17RPT04. [Online]. Available: https://www.euramet.org/research-innovation/search-research-projects/details/project/a-versatile-electrical-impedance-calibration-laboratory-based-on-digital-impedance-bridges
[38] R. D. Cutkosky and J. Q. Shields, "The precision measurement of transformer ratios," *IRE Trans. Instrum.*, vols. 1–9, no. 2, pp. 243–250, Sep. 1960.
[39] M. Miroslaw, J. Kaczmarek, and R. Rybski, "Characterization of PXI-based generators for impedance measurement setups," *IEEE Trans. Instrum. Meas.*, vol. 68, no. 6, pp. 1806–1813, Jun. 2019.
[40] S. Franco, *Design With Operational Amplifiers and Analog Integrated Circuits*, 4th ed. McGraw-Hill Education, 2014.
[41] *INRIM GitHub BClient Repository*. [Online]. Available: https://github.com/INRIM/BClient and https://github.com/INRIM/BClient/tree/main/LabWindows and https://github.com/INRIM/BClient/tree/main/Matlab
[42] L. Callegaro, "On strategies for automatic bridge balancing," *IEEE Trans. Instrum. Meas.*, vol. 54, no. 2, pp. 529–532, Apr. 2005. [Online]. Available: http://ieeexplore.ieee.org/document/1408226/
[43] BIPM, IEC, IFCC, ILAC, ISO, IUPAC, IUPAP, and OIML. (2011). *Evaluation of Measurement Data—Supplement 2 to the 'Guide to the Expression of Uncertainty in Measurement'—Extension to any Number of Output Quantities, JCGM 102:2011*. BIPM. [Online]. Available: https://www.bipm.org/en/publications/guides/gum.html
[44] BIPM. (2008). *Evaluation of Measurement Data—Supplement 1 to the 'Guide to the Expression of Uncertainty in Measurement'—Propagation of Distributions Using a Monte Carlo Method, JCGM 101:2008*. [Online]. Available: https://www.bipm.org/en/publications/guides/gum.html
[45] E. A. Walker, "The determination of magnitude and phase angle of electrical quantities," *Trans. Amer. Inst. Electr. Engineers*, vol. 60, no. 8, pp. 837–839, Aug. 1941.
[46] L. A. Marzetta, "An evaluation of the three-voltmeter method for AC power measurement," *IEEE Trans. Instrum. Meas.*, vol. IM-21, no. 4, pp. 353–357, Nov. 1972.
[47] F. Cabiati and G. C. Bosco, "CCE intercomparison of 10 mH inductors: Measurement method and results at IEN," Consultative Commitee Electr. (CCE), Tech. Rep. 92-52, 1992.
[48] F. Cabiati, G. C. Bosco, and A. Sosso, "Impedance comparison in the low-medium range through precision voltage measurements," in *Proc. 13th IMEKO World Congr.*, Turin, Italy, vol. 1, Sep. 1994, pp. 335–339.
[49] A. Muciek and F. Cabiati, "Analysis of a three-voltmeter measurement method designed for low-frequency impedance comparisons," *Metrol. Meas. Syst.*, vol. 13, no. 1, pp. 19–33, 2006.
[50] L. Callegaro and V. D'Elia, "A synchronized two-phase sinewave generator for AC metrology system compensations," *IEEE Trans. Instrum. Meas.*, vol. 49, no. 2, pp. 320–324, Apr. 2000.
[51] L. Callegaro and V. D'Elia, "Automatic compensation technique for alternating current metrology based on synchronous filtering," *Rev. Sci. Instrum.*, vol. 69, no. 12, pp. 4238–4241, 1998.
[52] L. Callegaro, V. D'Elia, and F. Manta, "A setup for linearity measurement of precision AC voltmeters in the audio frequency range," in *Proc. 16th IMEKO TC Symp.*, Florence, Italy, 2008, pp. 15–19.
[53] *Comité International des Poids et Mesures Mutual Recognition Arrangement*. [Online]. Available: https://www.bipm.org/en/cipm-mra
[54] *The CIPM MRA Database (KCDB)*. [Online]. Available: https://www.bipm.org/en/kcdb
[55] F. J. Wilkins and M. J. Swan, "Precision AC/DC resistance standards," *Proc. Inst. Elect. Eng.*, vol. 117, no. 4, pp. 841–849, Apr. 1970.
[56] G. Boella and G. M. Reedtz, "A room temperature setup to compare the quantized Hall resistance with 1-Ω standards," *IEEE Trans. Instrum. Meas.*, vol. 41, no. 1, pp. 59–63, May 1992.
[57] *BCR Intercomparison of AC Resistors*, Community Bur. Reference, Jul. 1989.
[58] H. Eckardt, *International Comparison of 10 mH Inductance Standards*, document CCE/95-36, Consultative Commitee for Electricity (CCE), 1995.
[59] L. Callegaro, V. D'Elia, and D. Serazio, "10-nF capacitance transfer standard," *IEEE Trans. Instrum. Meas.*, vol. 54, no. 5, pp. 1869–1872, Oct. 2005.
[60] L. Callegaro, V. D'Elia, F. Francone, and D. Serazio, "100 mH travelling standard for the EUROMET 607 pilot intercomparison," in *Proc. Conf. Dig. Conf. Precis. Electromagn. Meas.*, 2002, pp. 352–353.
[61] H. W. Lamson, "A new series of standard inductors," *Gen. Radio Experimenter*, vol. 27, no. 6, pp. 1–4, 1952.
[62] D. L. H. Gibbings, "A design for resistors of calculable AC/DC resistance ratio," *Proc. Inst. Elect. Eng.*, vol. 110, no. 2, pp. 335–347, Feb. 1963.

Martina Marzano was born in 1989. She received the master's degree in physics from the Università di Torino, Turin, Italy, in 2016, and the Ph.D. degree from the Politecnico di Torino, Turin, in collaboration with the Istituto Nazionale di Ricerca Metrologica, Turin, in 2020, with a focus on novel devices and methods for quantum resistance and impedance metrology.

From 2018 to 2019, she was a Guest Researcher for six months at the National Institute of Standards and Technology, Gaithersburg, MD, USA. As a Post-Doctoral Fellow with the Quantum Metrology and Nano Technologies Division, Istituto Nazionale di Ricerca Metrologica (INRIM), Turin. Her current research at INRIM is focused on the development and modeling of quantum Hall effect devices and measurement methods for impedance metrology.

Vincenzo D'Elia was born in 1965. He received the High School degree in electronics from the Technical School G. Plana, Turin, Italy, in 1988.

In 1996, he joined the Department of Electrical Metrology, Istituto Nazionale di Ricerca Metrologica (INRIM), Turin. He is currently with the Division of Quantum Metrology and Nano Technologies, INRIM, Turin. His current research interests include impedance, inductive voltage ratio, and low-current measurements.

Massimo Ortolano was born in 1969. He received the M.Sc. degree in electronic engineering and the Ph.D. degree in metrology from the Politecnico di Torino, Turin, Italy, in 1997 and 2001, respectively.

Since 2000, he has been an Assistant Professor with the Department of Electronics and Telecommunications, Politecnico di Torino, where he is in charge of several courses about electronic measurements. Since 2006, he has been collaborating with the Istituto Nazionale di Ricerca Metrologica (INRIM), Turin, with a focus on noise metrology, modeling of quantum Hall effect devices, and impedance metrology. His research interests include also fundamental constants, time and frequency metrology, and statistical methods for the evaluation of the uncertainty.

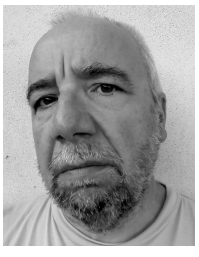

Luca Callegaro was born in 1967. He received the M.Sc. degree in electronic engineering and the Ph.D. degree in physics from the Politecnico di Milano, Milan, Italy, in 1992 and 1996, respectively.

He joined the Istituto Nazionale di Ricerca Metrologica (INRIM), Turin, Italy, in 1996, where he is currently the Head of the Quantum Electronics Group. He has authored about 100 articles on international reviews and the book *Electrical Impedance: Principles, Measurement and Applications* (Taylor & Francis, 2012). His research interest is focus on electrical impedance metrology. He is responsible for the Italian National standards of electrical capacitance, inductance, ac resistance, and ac voltage ratio.

Dr. Callegaro is a member, and served four years as the Chair of the Technical Committee for Electricity and Magnetism (TC-EM) of the European Association of National Metrology Institutes (EURAMET), and the Italian delegate to the Consultative Committee for Electricity and Magnetism (CCEM) of the International Committee for Weights and Measures (CIPM).

Open Access funding provided by 'Istituto Nazionale di Ricerca Metrologica - INRiM' within the CRUI CARE Agreement